Cell Communication & Adhesion

ISSN: 1541-9061 (Print) 1543-5180 (Online) Journal homepage: https://www.tandfonline.com/loi/icac20

# Role of E-Cadherin in Epithelial Architecture Maintenance

M. F. Izaguirre, D. Larrea, J. F. Adur, J. E. Diaz-Zamboni, N. B. Vicente, C. D. Galetto & V. H. Casco

**To cite this article:** M. F. Izaguirre, D. Larrea, J. F. Adur, J. E. Diaz-Zamboni, N. B. Vicente, C. D. Galetto & V. H. Casco (2010) Role of E-Cadherin in Epithelial Architecture Maintenance, Cell Communication & Adhesion, 17:1, 1-12, DOI: 10.3109/15419061003686938

**To link to this article:** https://doi.org/10.3109/15419061003686938

Published online: 30 Mar 2010.

*Cell Communication & Adhesion*, 17, 1–12, 2010

ISSN: 1541-9061 print / 1543-5180 online
DOI: 10.3109/15419061003686938

informa
healthcare

ORIGINAL ARTICLE

# Role of E-Cadherin in Epithelial Architecture Maintenance

M. F. Izaguirre, D. Larrea, J. F. Adur, J. E. Diaz-Zamboni, N. B. Vicente, C. D. Galetto and V. H. Casco

*Laboratorio de Microscopia Aplicada a Estudios Moleculares y Celulares, Facultad de Ingeniería (Bioingeniería-Bioinformática), Universidad Nacional de Entre Ríos, Entre Ríos, Argentina*

**Abstract**

Morphogenesis and architecture of a developing epithelium is controlled by both cell shape and contacts, mediated by spatially and temporally regulated cell adhesion molecules. The authors study if E-cadherin functions as a key factor of epithelial adhesion and epidermal architecture in vivo. They apply whole-mount digital deconvolution microscopy to evaluate three-dimensional (3D) E-cadherin expression during skin morphogenesis of Rhinella arenarum and in a cell adhesion alteration model. Results show morphogenetic changes in the 3D E-cadherin spatiotemporal expression pattern correlated with the increase of E-cadherin and in the number of cells with hexagonal geometry. Alterations in junction-protein phosphorylation showed drastic loss of E-cadherin and β-catenin in cell-cell contacts and the increase of cytoplasm and nuclear β-catenin in epidermis, suggesting the activation of the β-catenin signal pathway. Surprisingly, no changes in cell shape and skin architecture were registered, suggesting that epidermal E-cadherin appears to be involved in signaling rather than cell contact maintenance in vivo.

**Keywords:** anuran, cadherin, catenin, optical sectioning microscopy, skin



## INTRODUCTION

Epithelial cell adhesion depends on the intercellular interactions of transmembrane glycoproteins called cadherins, which form the basis of adherens junctions and desmosomes (Takeichi et al. 2000; Gumbiner 2000; Boggon et al. 2002). Cadherins represent the most important superfamily of $Ca^{2+}$-dependent adhesion molecules and should be considered as primary mediators of cell adhesion processes in vertebrates, and some also in invertebrates (Takeichi et al. 2000; Gumbiner 2000).

Specifically, E (epithelial)-cadherin has a role in normal state as well as in cancer invasion, metastasis, and other skin pathologies (Bonitsis et al. 2006; Waschke 2008). E-cadherin is functionally connected to the actin-cytoskeleton by catenins (Takeichi et al. 2000). In cadherin-catenin complexes, β-catenin or alternatively γ-catenin (commonly known as plakoglobin) binds directly to the carboxyl-end region of the cytoplasmic domain of cadherins (Wheelock et al. 1996; Kofron et al. 2002). α-Catenin links actin (Rimm et al. 1995) and α-actinin (Nieset et al. 1997) to β-catenin or plakoglobin (Wheelock et al. 1996). Additionally, $p120^{ctn}$ could regulate clusterization of cadherin/catenin complexes into the membrane plane by its direct association with the cadherin cytoplasmic-domain (Daniel and Reynolds 1995; Staddon et al. 1995).

Several studies suggest that the cadherin-actin binding/unbinding rate could change dynamically according to cellular type and cell-growth rate (Kofron et al. 2002). Additionally, catenins could be associated with products of tumor suppressor genes (Su et al. 1993), tyrosine-kinase receptors (Hoschuetzky et al. 1994), and tyrosine-phosphatase (Brady-Kalnay et al. 1995). Therefore, catenins are key elements in cell-cell adhesion regulation of cadherins and their cytoskeleton-interaction (Casco et al. 1998; Takeichi, 2000; Izaguirre et al. 2001a).

In vitro studies have shown that E-cadherin is not only necessary for adherens junction formation but its adhesive activity is also crucial for the assembly of other junctional complexes such as desmosomes, gap junctions, and tight junctions (Gumbiner et al. 1988; Watabe et al. 1994). These data suggest initial cell-cell adhesion mediated by the cadherin complex is a key step in setting up other cell junctions, cell polarity, and three-dimensional (3D) tissue organization. Surprisingly, in vivo studies suggest a signaling role rather than cell contact formation of E-cadherin in the stratified epithelium morphogenesis (Tunggal et al. 2005).

To study if E-cadherin functions as a key factor in epidermal epithelial adhesion and tissue architecture maintenance in vivo, we establish the *Rhinella arenarum*

Received 21 May 2009; accepted 5 February 2010
This work was supported by grants from SCYTFRH-UNER, PID 6082–1 (to V.H.C.) and PID 6088–1 (to M.F.I.).
Address correspondence to: M. F. Izaguirre, Laboratorio de Microscopia Aplicada a Estudios Moleculares y Celulares, Facultad de Ingenieria (Bioingenieria-Bioinformatica), Universidad Nacional de Entre Rios, CC 47, Suc. 3 (3100) Parana, Entre Rios, Argentina. E-mail: fizaguirre@bioingenieria.edu.ar

E-cadherin spatiotemporal pattern not only during normal epidermal morphogenesis but also in tadpoles treated with sodium orthovanadate ($Na_3VO_4$) to inactivate protein tyrosine phosphatases (PTPs), thus alterating the protein-phosphorylation level.

## MATERIALS AND METHODS

### Animals

Embryos and larvae were obtained according to Izaguirre et al. (2000) and were staged according to Gosner (1960). Stages 13, 15, 17, 19, 25, 35, 40, 42, and 46 were studied.

### Morphological Studies

Embryos (stages 13, 15, 17, 19, and 25), larvae (stages 35, 40, 42, and 46) and adult toad dissected skin of *Rhinella arenarum* were fixed and processed according to Izaguirre et al. (2001a). Specimens were cross-sectioned at 0.5-μm intervals with a Reichert Ultracut–S ultramicrotome, and sections were stained with toluidine blue. Images were recorded with an Apogee Instruments CCD camera, coupled to an Olympus BX-50 microscope.

#### *Epidermal Thickness Determination*

Serial cross-sections were performed for all developmental stages studied. Ten images were registered for each developmental stage using a 100× objective lens. Epidermis thickness was measured through cephalic and trunk regions using the Image-Pro Plus 5.1 software (Media Cybernetics) and their mean ± standard deviation was calculated. These data were used to establish the number of optical sections necessary to capture the whole specimen (see Optical Sectioning).

### Epidermal Expression of E-Cadherin and β-Catenin

#### *Antibodies*

Mouse monoclonal antibodies for E-cadherin (clone 36 mouse immunoglobulin G2a [IgG2a]; Transduction Laboratories, Lexington, KT) and rabbit policlonal antibodies for β-catenin (courtesy of Dr. Pierre McCrea, MD Anderson Cancer Center, University of Texas) were used at 1:50 and 1:100 dilutions in phosphate-buffered saline (PBS), respectively. We have previously demonstrated that these antibodies recognize anuran species (Izaguirre et al. 2000, 2001a, 2001b, 2006, 2008, 2009; Izaguirre 2003; Casco et al. 2000, 2006). Goat anti-mouse IgG-FITC (flourescein isothiocyanate) (Sigma, St.Louis, MO) and goat anti-rabbit IgG-Cy3 (Chemicon International) were used at 1:64 and 1:50 dilutions in PBS, respectively. Normal goat serum (NGS) (Vector Laboratories, Burlingame, CA) was used as negative control.

#### *Whole-Mount Immunofluorescence*

Embryos and larvae of *Rhinella arenarum* were fixed in toto in Carnoy solution for 2 h at room temperature (RT). These were washed in PBS and permeated for 1 h in 1% Triton X-100/PBS. Animals were washed in PBS and incubated in NGS for 45 min, followed by 1.5 h incubation with primary antibodies at 37°C, washed in PBS, and incubated with species-specific FITC and Cy3 secondary antibodies for 2 h at RT in darkness. Finally, animals were rinsed in PBS in darkness and mounted with Vectashield (Vector) mounting-medium.

#### *3D E-Cadherin Expression Determination by Digital Deconvolution Microscopy (DDM)*

Five animals of each model were optically sectioned with a 100× objective lens at 0.25 μm intervals (*z*-axis) with a system developed by us based on an Olympus BX-50 epifluorescence microscope and an Apogee Instruments CCD camera (Adur and Schlegel 1997; Diaz-Zamboni 2004; Adur 2006; Adur et al. 2007; Diaz-Zamboni et al. 2007). According to skin thickness determined in the morphological study, Z-series of 128 optical sections of $512 \times 512$ pixel$^2$ were collected. Optical section intervals are set in accordance to the Nyquist sampling theorem (Castleman, 1996). Afterwards, images were cut to $256 \times 256$ pixel$^2$ using the MATLAB program (MathWorks), in order to reduce computer resource consumption.

The morphometric study determined that the epidermis of stage 19 *Rhinella arenarum* larvae has an average thickness of 18.79 ± 5.08 μm (see Table 1). Thus, using a 100× lens and moving at 0.25-μm intervals, we can completely scan the epidermis with 128 optical sections (32 μm). The dimensions and number of the optical sections are in relation with the deconvolution algorithm employed, which uses the fast Fourier transform (FFT), which in turn requires that input data have dimensions of $2^n$ (2, 4, 8, 16, 32, 64, 128, 256, 512, etc.).

Exposure time was determined experimentally to register 8-bit images with the best contrast and avoiding intensity saturation. Data of specific immunofluorescence (*f*) versus background (*b*) were obtained using the

**Table 1.** Epidermal thickness throughout *Rhinella arenarum* developmental stages

| | St. 13 | St. 15 | St. 19 | St. 25 | St. 35 | St. 40 | St. 42 | St. 46 | Adult |
|---|---|---|---|---|---|---|---|---|---|
| Mean ± *SD* (μm) | 32.8±1.3 | 21.9±4.7 | 18.8±5.1 | 12.3±1.9 | 10.1±1.1 | 17.0±0.7[1]<br>26.7±6[2] | 13.7±1.8 | 14.3±1.1 | 69.8±8.4 |

[1]Bistratified prometamorphic skin. [2]Multistratified metamorphic skin. At stage 40, bistratified prometamorphic skin coexists with the new multistratified metamorphic skin.

SUMDD software (Diaz-Zamboni 2004; Diaz-Zamboni et al. 2007). Because each developmental stage was captured at a different exposure time, the fluorescence indexes were calculated ($I_f$):

$$I_f = \frac{f}{b.t_{\text{exposure}}}$$

Afterwards, the raw images were deconvolved to restore out of focus fluorescence to its correct spatial position (Diaz-Zamboni et al. 2007). Because blurring is a function of the optical setup of the microscope (mainly of the objective lens), it can be modeled with algorithms derived from the mathematical analysis of the image formation process. This process is represented by the 3D convolution (⊗) of a known variable, the 3D PSF (point spread function) or PSF($x$, $y$, $z$), and an unknown variable, the 3D distribution of fluorescence in the specimen o (x, y, z) (Castleman 1996; Jansson 1997; McNally et al. 1999). The simplest form of the mentioned phenomenon is mathematically described by the equation:

$$i\,(x, y, z) = PSF\,(x, y, z) \otimes 0\,(x, y, z)$$

where $i$ ($x$, $y$, $z$) is the 3D image obtained by optical-sectioning.

In this particular work, a constrained iterative deconvolution method was used (Diaz-Zamboni et al. 2008).

Finally, using the SUMDD, 3D E-cadherin immunofluorescence pattern was rebuilt employing maximum intensity projections of raw and deconvolved image stacks. Additionally, the two-dimensional (2D) β-catenin expression pattern throughout development (stages 13, 15, 17, 19, 25, 35, 40, and 46) was determined to match the E-cadherin–β –catenin adhesion model.

### Disruption of Cell Adhesion Mediated by E-Cadherin–β-Catenin

To evaluate the regulation of the 3D E-cadherin adhesive pattern in skin, a model of PTP inhibition (by $Na_3VO_4$) was implemented.

#### *Bioassay*

Stage 35 larvae were incubated for 24 h in 1 mM $Na_3VO_4$ (Sigma St. Louis, MO) solution and laboratory artificial water (control), at a 10 larvae/L density, 20°C ± 2°C and 12-h light:12-h dark photoperiod. Bioassays were performed by triplicate. Preliminary bioassays showed 100% survival in the above mentioned conditions.

#### *Immunofluorescence and Morphological Studies*

At the 24 h of bioassay, control and $Na_3VO_4$-treated animals were fixed and processed as mentioned above to carry out the 3D E-cadherin expression quantification, 2D β-catenin expression pattern establishment, and morphological analysis.

### Epidermal Cell Morphology: Relationship With Mechanic Stabilization and Contact Remodeling

In order to evaluate adhesive-contact remodeling mediated by E-cadherin throughout skin development and in the cell-cell adhesion alteration model via $Na_3VO_4$, cell morphology and cross-sectional area were evaluated.

The cell morphology of 2D images from five specimens for each developmental stage and $Na_3VO_4$-treated animals ($n = 5$) was analyzed. Cell geometry was classified in round cells and 4-, 5-, 6-, 7-, 8-, and 9-sided cells. Additionally, using Image-Pro Plus, the cross-sectional area of 4-, 5-, 6-, and 7-sided cells was calculated to determine if growth or shrinkage of individual cell contacts is a result of local neighbor exchanges or de novo synthesis of E-cadherin.

### Statistical Analysis

Differences in 3D E-cadherin expression in different stages were analyzed statistically by Analysis of variance (ANOVA) test with Tukey's test. 3D E-cadherin expression between head and trunk was compared by $t$ test. Differences in mean cellular morphology were analyzed statistically by nonparametric Kruskal-Wallis ANOVA test with Dunn test. Differences in mean cellular area were analyzed statistically by $t$ test and nonparametric Mann-Whitney test. Values of $p \leq .05$, $p \leq .01$, and $p \leq .001$ were considered significant, very significant, and extremely significant, respectively. Data were analyzed with SPSS 10.0 and plotted with SigmaPlot 2001 softwares.

## RESULTS

### E-Cadherin Expression During Skin Morphogenesis of *Rhinella arenarum*

E-cadherin expression was principally detected for the first time in epidermal ectoderm near regions of neural folds at stage 15, showing some cells began displaying localized E-cadherin protein in a discontinuous, linear pattern along a subset of cell boundaries (Figure 1a). At stage 17, triangular-shaped regions of high immunofluorescence (immature puncta) appeared (Figures 1b and 2a), which became dot-shaped at stage 19 and stay established where three to four cells met (Figure 1c). DDM images clearly shows more continuous E-cadherin patterns in all cell perimeters (Figure 2a, b). No differences in the location pattern were detected in the cephalic and trunk regions (not shown).

Statistical analysis demonstrated that 3D E-cadherin expression level in dorsal skin increases throughout development (Figure 3a). In the cephalic region, a significant increase occurred from stages 17 to 19, and an extremely significant increase occurred from stages 19

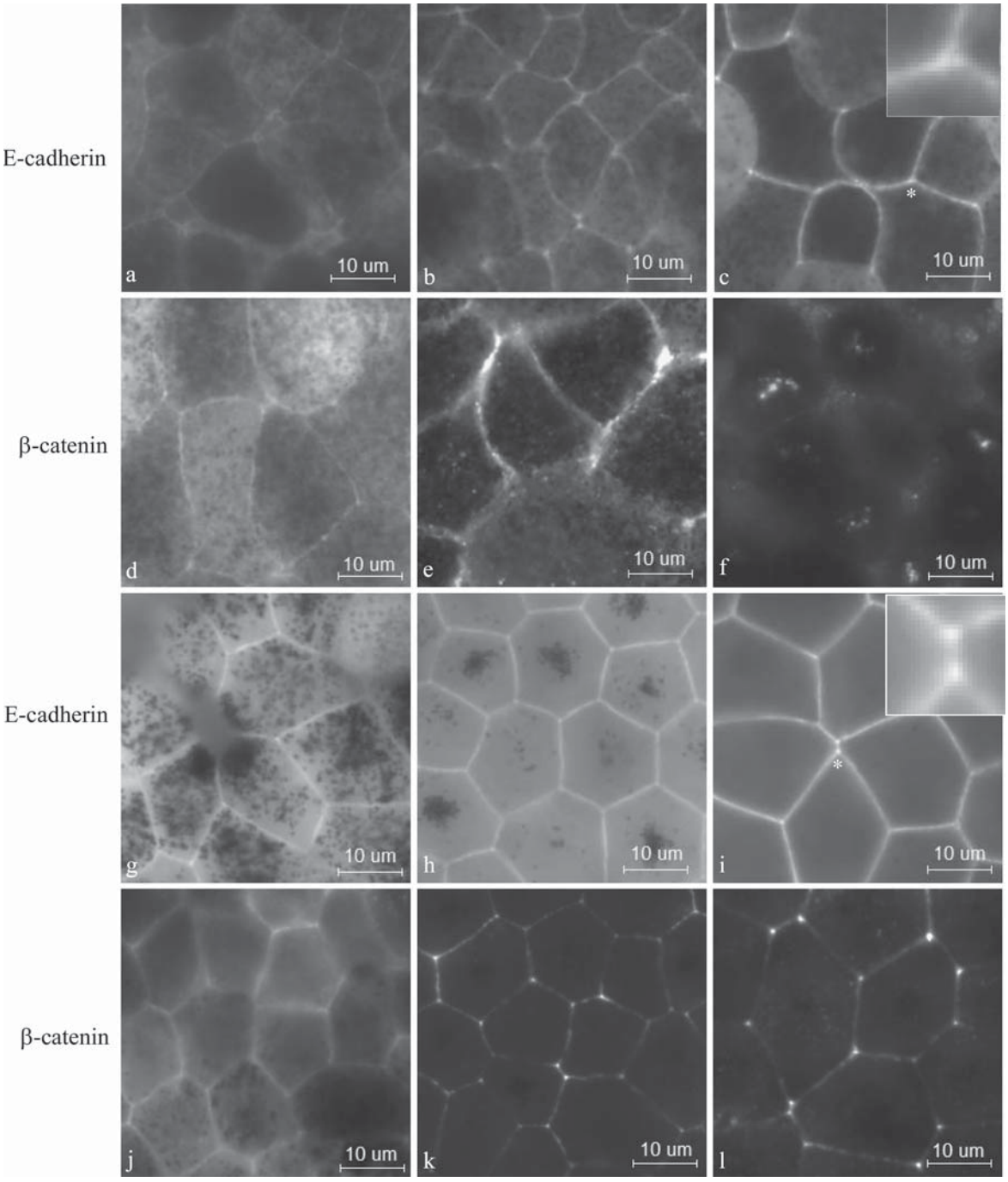


**Figure 1.** 2D E-cadherin and β-catenin expression of dorsal epidermis of *Rhinella arenarum* (nondeconvolved images). (**a**) Stage 15; (**b**, **d**) stage 17; (**c**, **e**, **f**) stage 19; (**g**, **j**) stage 25; (**h**, **k**) stage 35; (**i**, **l**) stage 40. Asterisk (*) marks the punctum shown in more detail.

to 35. From stages 35 to 40, an increased tendency was observed yet the differences were nonsignificant (Figure 3a). However, the increase in expression level at stage 40 was extremely significant compared to stages 17, 19, and 25. 3D E-cadherin expression at stage 46 could not be quantified because the signal was possibly masked by autofluorescence, due to increased skin thickness and the presence of high-fluorescence-intensity endogenous pigments. Additionally, a significant and a very significant increase of expression level between cephalic and trunk regions were verified in stages 25 and 35, respectively; however, E-cadherin expression of trunk dorsal epidermis at stages 15 and 17 was extremely low and therefore nonquantifiable. In the trunk region, a very significant increase in E-cadherin expression was registered from stages 19 to 40 (Figure 3a).

From stages 25 onwards, puncta remodel into higher molecular density dot-shaped zones, additionally with an accumulation in cell boundaries of E-cadherin, correlating with an increase in expression level (Figures 1g–i, 2c–e). It was noted that from stage 25 onwards, autofluorescence increased due to increased larval pigmentation, but did not interfere with specific immunosignal (Figures 1g–i, 2c–e). Particularly, and for unknown reasons, autofluorescence is higher at stage 35 than stage 40 (Figures 1h, i, 2d, e).

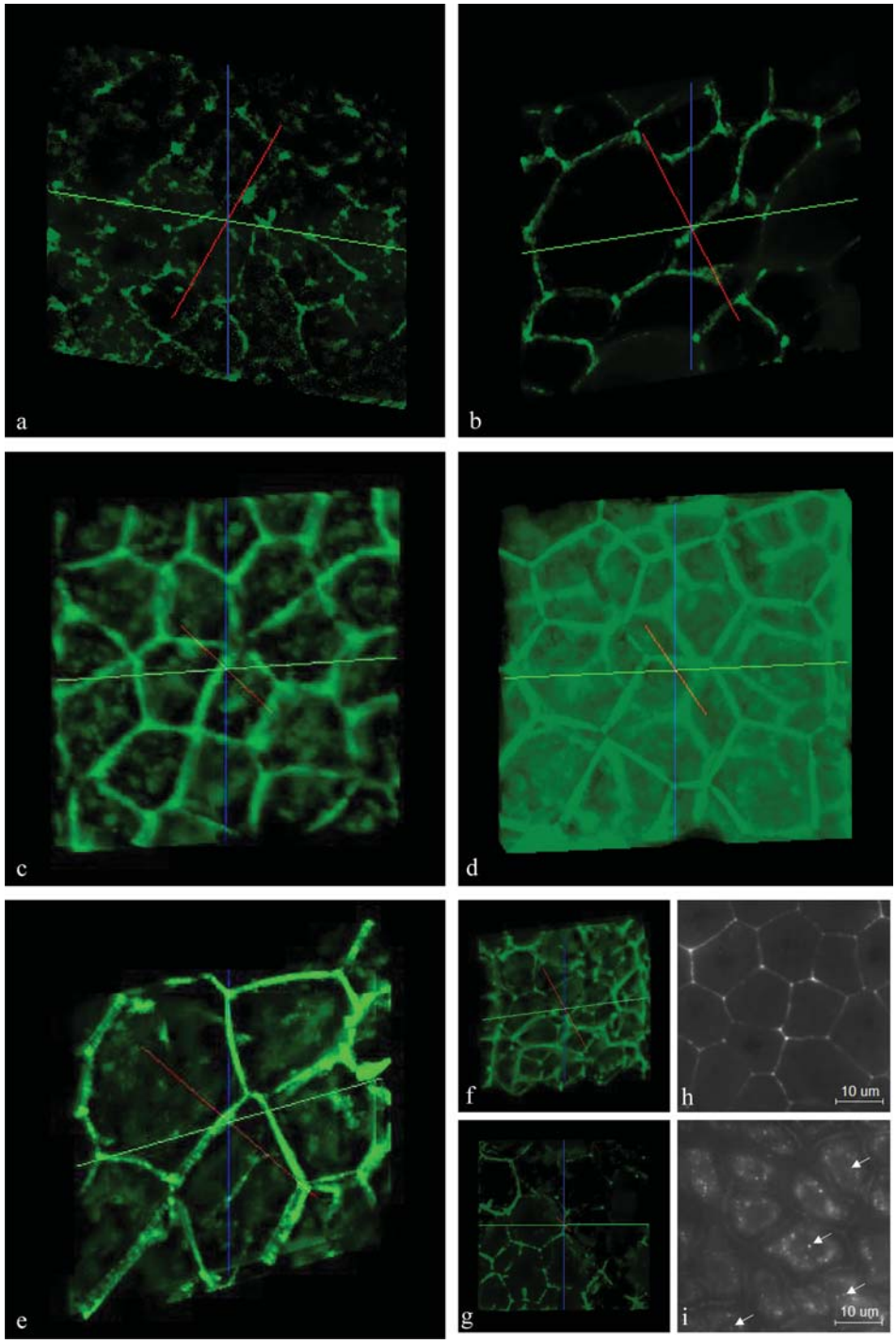


**Figure 2.** (**a**–**g**) 2D maximun intensity projections of 128-image stacks of E-cadherin of cephalic dorsal epidermis of *Rhinella arenarum*. (**a**–**e**) DDM images clearly show that E-cadherin increases in cell boundaries, switching from a dotted to a continue pattern during development, with high immunosignal density in puncta. Stage 17 (**a**), stage 19 (**b**), stage 25 (**c**), stage 35 (**d**), and stage 40 (**e**). All stacks include two cell layers; panel (**d**) looks different from the other panels because when tadpoles developed, their pigment quantity increased. Intriguingly, autofluorescence from pigments is higher at stage 35 than any another stage (**a**–**e**). (**f**, **g**) $Na_3VO_4$-treated tadpoles show a progressive time-dependent decrease in E-cadherin expression. For unknown reasons, treated-tadpoles became unpigmented, thus decreasing autofluorescence (**f**, **g** versus **d**). (**h**, **i**) 2D β-catenin expression of cephalic dorsal epidermis of control (**h**) and $Na_3VO_4$-treated (**i**) Stage 35 larvae skin. Clearly, β-catenin disappears from cell boundaries andincreases at cytoplasmic and nuclear level, suggesting a signaling role. Lines represent: *x*-(green), *y*- (blue), and *z*- (red) axes.

## E-Cadherin Expression After Cell-Cell Adhesion Alteration

E-cadherin expression pattern in ***Rhinella arenarum*** dorsal skin of $Na_3VO_4$-treated stage 35 larvae showed great differences with control stage 35 larvae (Figure 2d, f, g).

E-cadherin expression in $Na_3VO_4$-treated epithelium drastically decreased, both in the cephalic and trunk regions (Figure 3b). Additionally, a progressive change in cell-cell junction organization mediated by E-cadherin was detected (Figure 2f, g), showing increased segmentation in the expression pattern, loss of this molecule in

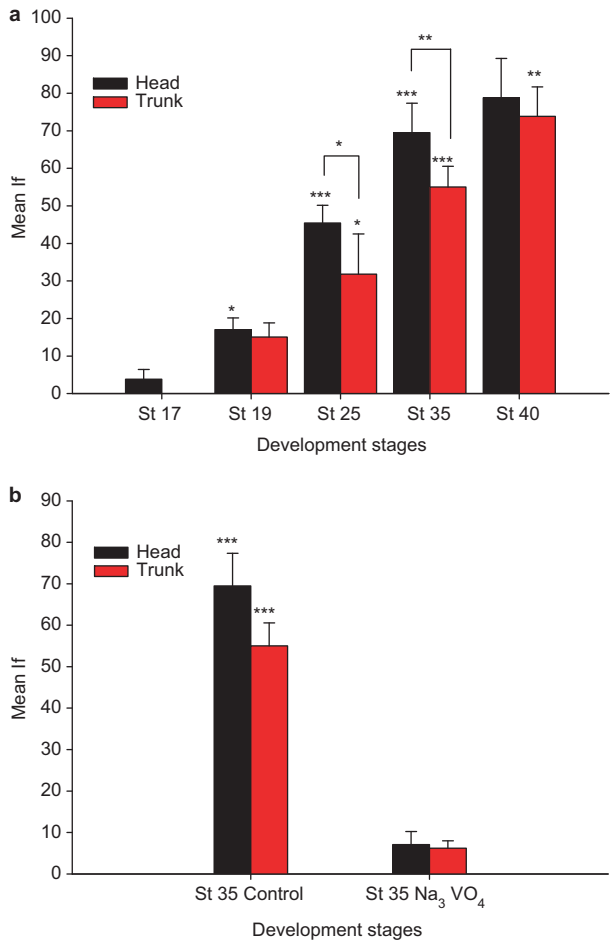


**Figure 3.** 3D E-cadherin expression of cephalic and trunk dorsal epidermis throughout development of *Rhinella arenarum* (**a**) and after treatment with $Na_3VO_4$ (**b**). ***$p \leq .001$; **$p \leq .01$; *$p \leq .05$.

some cell boundaries, and preservation of puncta. In some regions, puncta appear smaller and apparently disconnected from cellular-membrane molecules (Figure 2d, f, g). Immunolocalization was mainly observed on the lateral membrane of the superficial ectodermal cells, whereas for cells in the deep-ectodermal layer a very diffuse immunosignal was observed. No significant differences in 3D E-cadherin expression between cephalic and trunk regions of $Na_3VO_4$-treated larvae were found (Figure 3b). Intriguingly, larvae treated with $Na_3VO_4$ became less pigmented, which reduced autofluorescence.

Morphological studies do not show clear differences between control and Na3VO4-treated larvae, suggesting preservation of cell morphology and epithelial architecture in a 24 h. treatment (Figure 4).

## 2D β-Catenin Expression Throughout Development

To corroborate the cell-cell adhesion alteration model generated, the 2D β-catenin expression pattern was determined (Figure 1d–f, j–l). β-Catenin was scarcely detected at stage 17 and was regionally coexpressed with E-cadherin in outer-ectoderm cell membranes of dorsal (Figure 1d) as well as ventral skin (not shown). At stage 19, β-catenin expression increases and presents higher intensity in puncta (Figure 1e). Additionally, β-catenin was detected in puncta in cytoplasmic and/or nuclear level in deeper imaging planes that include the nucleus (Figure 1e, f). At stages 25 and 35, β-catenin was mainly detected at submembrane level, in the outer-ectoderm layer in cell-cell junctions at a depth just below the apical membranes, in the superficial ectodermal layer, and with increased intensity in puncta (Figure 1j, k). At the beginning of metamorphosis (stage 40), no changes were detected with respect to stage 35 larvae (Figure 1l). Due to an increase in epidermal thickness and impermeability of stage 46 larvae, specific immunosignal was not clearly detected (not shown).

## β-Catenin Expression in $Na_3VO_4$-Treated Larvae

The cephalic and trunk dorsal skin β-catenin pattern of stage 35 $Na_3VO_4$-treated larvae was significantly different

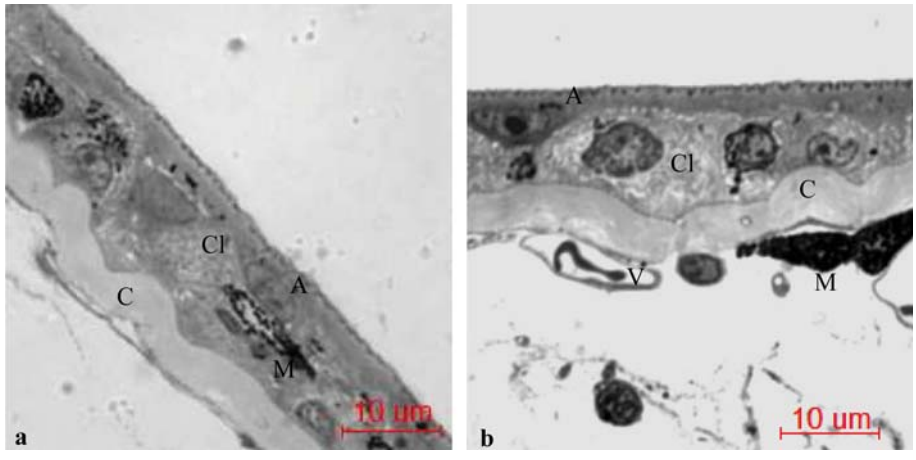


**Figure 4.** Sagital sections of $Na_3VO_4$-treated (**a**) and control (**b**) stage 35 larvae skin of *Rhinella arenarum*. Toluidine blue stain. No morphological changes after $Na_3VO_4$ treatment were detected. A: apical cell; Cl: clear cell; C: collagen; M: melanophore; V: sanguine vessel.

to that of control larvae (Figure 2h, i). Expression was predominantly cytoplasmic, presenting a ring-like pattern lining the plasma membrane and with some nuclear localization (arrows, Figure 2i). Despite a noticeable increase in cytosolic β-catenin in $Na_3VO_4$-treated larvae epidermal cells, an increase in nuclear β-catenin was less evident. However, this does not preclude the increased nuclear activity of β-catenin and would require further testing. Additionally, submembrane signal was extremely diffuse and it was not detected in puncta (Figure 2i).

### Epidermal Cell Morphology: Relationship With Mechanic Stabilization and Contact Remodeling

In all studied stages the predominant cell type was that of 5-sided and 6-sided cells, together they make up approximately 50–60% of total cells in stages 15, 17, and 19 and 70–80% in stages 25, 35, and 40 (Figure 5a). As development progressed the hexagonal cell amount increased (Figure 5a). Additionally, round cells detected at stage 17 disappear at stage 25, together with an important increase of the amount of 7-sided cells from stage 35 onwards.

Statistical analysis detected significant differences only between 5- and 6-sided cells at both stages 15 and 25 (Figure 5a). However, $Na_3VO_4$-treated animals did not show significant differences in the relative amount of cellular types, suggesting that there were no changes in cell morphology after 24 h of treatment (Figure 5b).

In order to study how cell contacts were remodeled, we evaluated cell cross-sectional area together with changes of E-cadherin and β-catenin expression throughout development. Specifically, we analyzed if molecules accumulated inside the cell derived from preexistent cell contacts rather than from the biosynthetic pathway.

Measuring cell areas during the elongation of the boundary, when cells change their cross-sectional geometry, revealed that areas fluctuate throughout development, showing extremely significant increase at stage 19 and stage 40 from pentagons to hexagons, and at stage 35 from pentagons to hexagons and to heptagons (Figure 6a). These data, correlated together with the increase in E-cadherin and β-catenin expression, suggest that the

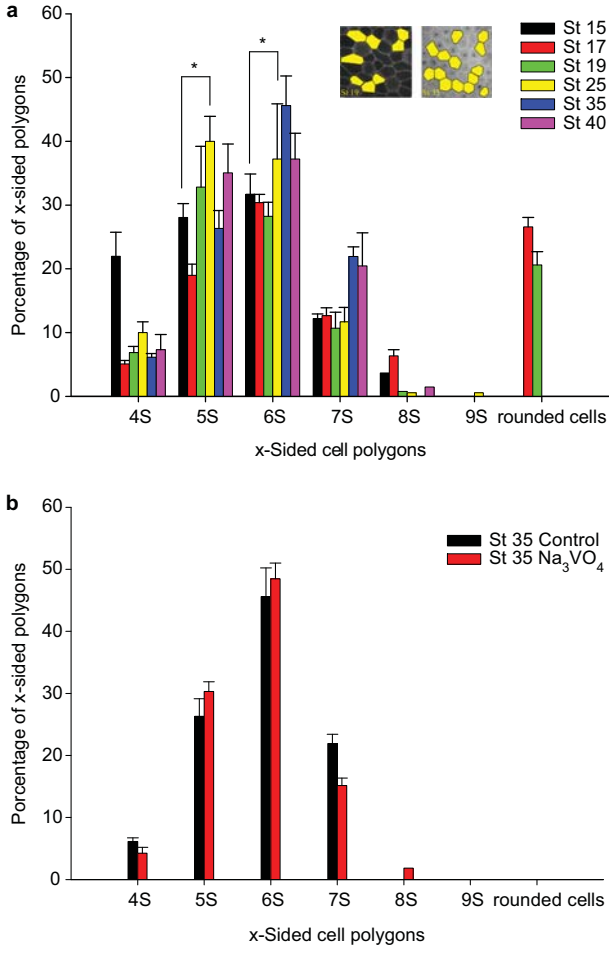


**Figure 5.** Morphology of *Rhinella arenarum* apical epidermal cells, throughout the development (**a**) and in stage 35 $Na_3VO_4$-treated larvae (**b**). *$p \leq .05$. Panel (**a**) clearly shows that the amount of the hexagonal cells increases throughout development; inserts show stage 19 versus stage 35.

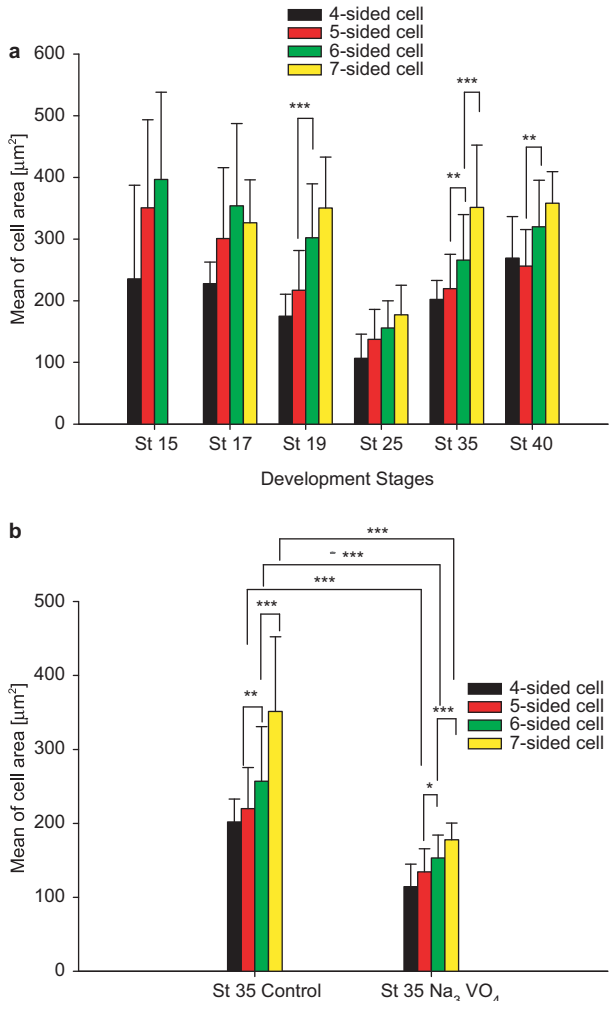


**Figure 6.** Skin cell cross-sectional area of *Rhinella arenarum*, throughout the development (**a**) and in stage 35 $Na_3VO_4$-treated larvae (**b**). *$p \leq .05$; **$p \leq .01$; ***$p \leq .001$.

formation of new cell contacts may use material derived from new biosynthesis instead of material derived from preexistent contacts (Figure 6a). Round cells and octagons were discarded for the analysis. Larvae treated with $Na_3VO_4$ showed a significant and a extremely significant increase of the cell area from pentagons to hexagons and from hexagons to heptagons, respectively (Figure 6b). In contrast, cell area of pentagons, hexagons, and heptagons of $Na_3VO_4$-treated stage 35 larvae significantly decreased with respect to those of control larvae (Figure 6b).

## DISCUSSION

Adhesion mediated by the cadherin-catenin complex is pivotal for the development of multicellular organisms. Features such as a large repertoire of homotypically interacting cadherins, rapid assembly and disassembly, and a connection to a force-generating actin cytoskeleton make cadherin-mediated junctions ideal structures for the execution of complex changes in cell and tissue morphology during animal development and maintaining of tissue architecture.

It is known that E-cadherin expression is down-regulated or absent in tissue architecture remodeling as well as in tumor invasion and metastasis (Vleminckx et al. 1991; Perl et al. 1998). Therefore, in the present article the role of 3D E-cadherin expression in regulating cell morphology and epithelial architecture maintenance is discussed in some detail using as models of epithelial remodeling the anuran metamorphosis and changes at the phosphorylation level of E-cadherin–β-catenin complexes.

DDM studies employed in the present work allowed us to quantify the epidermal E-cadherin expression from stage 17 to stage 40, showing deep changes in the expression pattern of intercellular junctions associated with *Rhinella arenarum* development. A transition from dot to nonsegmented lines and an increase in the adhesive belt thickness, puncta size, and molecular density were observed. Maximum intensity projections of raw and deconvolved stacks suggest that during *Rhinella arenarum* epidermal morphogenesis, E-cadherin establishes exploring contacts at stage 15, transient contacts that increase from stage 17 onwards, and it turns into a zippering framework structure from stage 25 onwards, which coincides with the transition from embryonic to larval life, as was postulated by Izaguirre (2003). From stage 25 onwards, this framework increases and becomes organized in puncta in the union of two or more cells.

Functionally, the quick disassembly and the light force associated at cadherin EC1 (extracellular cadherin repeat domain 1) interaction could be advantageous in the early exploration phase of junctional remodeling that must occur during the establishment of the first tissue patterns (Perret et al. 2004; Pokutta and Weis 2007). Afterwards in the development, the continuous pattern and puncta observed could represent steady contacts, where the interaction between all cadherin-ectodomains should generate the force to be able to stabilize the new tissue structure formed, which must support the strong tensions to resist to deformation (Kusumi et al. 1999; Perret et al. 2004; Bayas et al. 2006). Similar results have been found using in vitro systems (McNeill et al. 1993; Angres et al. 1996; Adams et al. 1996, 1998).

Unfortunately, 3D E-cadherin expression at the end of metamorphosis could not be evaluated by DDM. Several factors could affect the visualization by whole-mount immunofluorescence: impenetrability of antibodies due to the impermeability of the skin's outer stratus and its increased thickness, and because the plasma membrane of cornified cells became thick by the deposition and cross-linking of proteins to build the insoluble cornified envelope (Steinert and Marekov 1999). Additionally, an increase in autofluorescence due to increased pigmentation produced confusing results because of our system's technical limitations. However, Izaguirre (2003) established that even though a drastic skin remodeling by the disassembling and reassembling of adhesive contacts is produced at the metamorphic climax in *Rhinella arenarum*, E-cadherin expression in cell boundaries is stable. Moreover, several studies carried out in *Xenopus laevis* (Levi et al. 1991), mouse (Tunggal et al. 2005), and human (Jensen et al. 1997; Moles and Watt, 1997) show that E-cadherin is present in all epidermal layers and exocrine ducts, but decreases in the corneal stratus when cells become keratinized. Surprisingly, a high signal of E-cadherin is maintained during skin remodeling (Izaguirre et al. 2001a; Izaguirre 2003), when live larval, apoptotic larval, and live preadult cells coexist and there is higher adhesive contact remodeling to replace larval with preadult skin.

Whole-mount immunofluorescence together with DDM allowed us to detect E-cadherin in earlier *Rhinella arenarum* developmental stages than those reported previously (Izaguirre et al. 2000; Izaguirre 2003). $Na_3VO_4$ is an inhibitor of PTP that significantly reduced E-cadherin and β-catenin protein levels at cell contacts and also produced an increase in cytosolic and nuclear β-catenin. 3D representations of the E-cadherin pattern in the altered larval skin strongly suggest that in spite of its dramatic decrease in cellular boundaries and of the β-catenin rate of association to membrane, epithelial cells preserve E-cadherin in puncta trying to maintain cell shape, thus suggesting that no major changes in adherens junction formation mediated by E-cadherin and cadherin-associated β-catenin take place.

It is known that the strong adhesion formation by cadherins depends on their association with the actin-cytoskeleton, a connection mediated by α- and β- or γ-catenin (Wheelock et al. 1996). Several studies have demonstrate that the phosphorylation of β-catenin reduces their affinity for E-cadherin by approximately 85%(Xu and Kimelman 2007) and increases the free cytosolic pool of β-catenin, regulating its function as a signaling molecule during epithelial cell migration (Muller et al. 1999). Additionally, it is known that to

maintain β-catenin associated to cadherin in a reasonably stable manner, it is necessary both to maintain a pool of β-catenin in a dephosphorylated state as well as low levels of free cytoplasmic β-catenin (Miller and Moon 1996). This can be accomplished by having PTP active, and excess free phosphorylated β-catenin is targeted to β-catenin destruction multiprotein complexes, which include such proteins as axin, APC, PP2, GSK3β, and CK1α (Willert and Jones 2006; Xu and Kimelman 2007).

Several studies using PTP nonselective inhibitors, such as vanadate or $Na_3VO_4$, have generated conflicting results. In some studies, tyrosine phosphorylation of zonula adherens proteins, especially β-catenin, is not associated with the disruption of the cadherin-actin cytoskeleton linkage, zonula adherens disassembly (Esser et al. 1998), or increase of the transepithelial permeability (Young et al. 2003), whereas other studies do find the disassembly of adherens junctions (Hazan and Norton 1998; Chen et al. 2007).

Mechanism(s) by which the tyrosine phosphorylation state of one or more zonula adherens proteins can, through in-to-out signaling, regulate cadherins is poorly understood. Interestingly, PTP inhibition alone promotes tyrosine phosphorylation of zonula adherens proteins, coincident with increases in the movement of macromolecules and neutrophils across the endothelium barrier (Young et al. 2003). Opening of the paracellular pathway theoretically permits disengagement of homophilically bound VE (vascular endothelial)-cadherin ectodomains and lateral mobility in the lipid bilayer with redistribution across the plasma membrane. It is conceivable that as VE-cadherin and either β- or γ-catenin leave the intercellular junctions, they do so together as a VE-cadherin–catenin complex. This would permit more dynamic and efficient zonula adherens disassembly/reassembly in response to rapidly changing physiological demands (Young et al. 2003).

In the present work, neither disassembly of cell junctions nor histological changes were observed, but $Na_3VO_4$ significantly modified both 3D and 2D expressions of E-cadherin and β-catenin, respectively. The expression patterns found suggest that the epithelial cells gradually revert the pattern established throughout development; thus, cells decrease E-cadherin and submembrane β-catenin, present a segmented immunofluorescence cell-lining pattern, and preserve E-cadherin in puncta to maintain cell shape, and additionally increase cytosolic and nuclear β-catenin as mediator of signaling. The histological study did not reveal blistering or loss of cellular shape or tissue architecture, suggesting neither major changes nor major role in cell contact formation and/or maintaining in vivo of E-cadherin. Maybe, E-cadherin loss was compensated by the transcriptional up-regulation of other adhesive molecules avoiding cell-cell contact disorganization, such as has been suggested by Roitbak et al. (2004). Interestingly, it has been recently reported that E-cadherin gene inactivation in mouse produces perinatal death due to the inability to maintain a functional epidermal water barrier, and revealed that the key tight junctional components were improperly localized, resulting in altered tight junctional architecture and epidermal resistance (Tunggal et al. 2005). Surprisingly, desmosomes were formed normally and no obvious defects in cell contacts were detected, suggesting that E-cadherin is specifically required for tight junctions but not for the formation of other contacts; this apparently involves signaling rather than cell contact formation in vivo (Tunggal et al. 2005).

These results suggest that other adhesion molecules switch roles with E-cadherin to avoid cell-cell contact disorganization or that E-cadherin's role is mainly confined to cell signaling. On the other hand, internalization and recycling of cadherins has recently emerged as a major route for controlling adherens junction remodeling and maintenance (Fujita et al. 2002; Palovuori et al. 2003). There is evidence that a small pool of cell surface E-cadherin is constitutively and constantly trafficked through endocytosis and recycling, and this pool increases markedly in preconfluent cells and when cell-cell contacts are weakened or disrupted by distinct mechanisms (Fujita et al. 2002; Palovuori et al. 2003). In contrast, in the present work, no increase in cytosolic E-cadherin was detected. Therefore, we suggest that E-cadherin is internalized and then shuttled to lysosomes instead of being recycled back to the lateral membrane. Lysosomal targeting of E-cadherin is an important posttranscriptional mechanism to deplete cellular E-cadherin during Src-induced epithelial to mesenchymal transitions (Palacios et al. 2005).

In order to evaluate how cell contacts are remodeled throughout development, we measure cross-sectional cell area in normal specimens and specimens affected by cadherin-catenin complex deregulation by PTP inhibition. The increase in average area of 4-, 5-, 6-, and 7-sided cells and E-cadherin and β-catenin expression suggest that cells must synthesize E-cadherin and β-catenin to contribute in the formation of new contacts, independently of utilization of material derived from preexisting contacts.

Epidermal morphological changes (not shown) during development, together with the beginning of E-cadherin expression in *Rhinella arenarum* from stage 15 until stage 25, show that a strong remodeling of cell shape and polarization of cytoplasm components is produced. In this way, pigments assume an apical localization, lipid droplets become situated in the intermediate area, and yolk-bodies move to the basal region. Similar polarization events in the apical epithelial cells take place during *Xenopus laevis* embryogenesis (Billett and Gould 1971). Both in vitro and in vivo studies have shown that E-cadherin is not only necessary for adherens junction formation, but also that its adhesive activity is crucial for the assembly of other junction complexes. This assembly is correlated with the establishment of cell polarity and with the recruitment of protein complexes essential for

cell polarity set up in cell junctions, such as E-cadherin and associated proteins (Lecuit 2005; Tunggal et al. 2005; Classen et al. 2005; Wang and Nathan 2007).

In conclusion, present results suggest that during skin development, epithelial cell geometry varies to reach higher physical stability in order to support greater tensions, therefore increasing the proportion of hexagonal cells. Coincidentally, E-cadherin expression increases, suggesting it has a role in controlling cell shape and thus in epithelial architecture stabilization. Low levels of E-cadherin–β-catenin complex phosphorylation are essential to the maintenance of these complexes, but are not crucial to maintain in vivo skin architecture.

The preservation of tissue architecture resulting from the alteration of the E-cadherin-ß-catenin complexes by phosphorylation, clearly suggests that the compensatory adhesion systems must be up-regulated and at the same time E-cadherin must be down-regulated to maintain the epithelial architecture. ß-catenin depletion in the plasma membrane and its predominant cytoplasmic location in epidermal cells of Na3VO4-treated larvae, suggest that it would be difficult for a member of the cadherin family to replace E-cadherin, as has been found in the autosomal dominant polycystic kidney disease (ADPKD) (Roitbak et al., 2004). However, this hypothesis is seen to be improbable because it has been demonstrated that cadherin-catenin systems are essential to maintain not only adherens junction but also structurally intact occludens zonula and epithelial permeability barrier (Price et al. 2002). Therefore, β-catenin withdraw from their normal position at the basolateral membrane after PTP inhibition and their increase in the cytoplasm could wait for another cadherin to replace E-cadherin function, after 24 h of $Na_3VO_4$ treatment. Future experiments will be necessary to clarify the last hypothesis.

***Declaration of interest:*** The authors report no conflicts of interest. The authors alone are responsible for the content and writing of the paper.

## REFERENCES


Adams CL, Chen YT, Smith SJ, Nelson WJ (1998). Mechanisms of epithelial cell-cell adhesion and cell compaction revealed by high-resolution tracking of E-cadherin-green fluorescent protein. *Cell Biol.* 142: 1105–1119.

Adams CL, Nelson WJ, Smith SJ (1996). Quantitative analysis of cadherin-catenin-actin reorganization during development of cell-cell adhesion. *J Cell Biol.* 135: 1899–1911.

Adur J (2006). Determinacion de las propiedades opticas de un sistema de epifluorescencia y su utilizacion en estudios de microscopia cuantitativa de 3D. Tesis de Maestría (Inedita). Facultad de Ingenieria, Universidad Nacional de Entre Rios, Argentina.

Adur JF, Diaz-Zamboni JE, Vicente NB, Izaguirre MF, Casco VH (2007). Digital deconvolution microscopy: Development, evaluation and utilization in 3D quantitative studies of E-cadherin expression in skin of Bufo arenarun tadpoles. In: *Modern Research Educational Topics in Microscopy,* Mendez-Vilas A and Diaz J (eds.). Spain, pp. 906–916.

Adur JF, Schlegel JO (1997). Diseno, desarrollo y construccion de un sistema de avance micrometrico para microscopios fotonicos. Tesis de Grado (Inedita), Facultad de Ingenieria, Universidad Nacional de Entre Rios, Argentina.

Angres B, Barth A, Nelson WJ (1996). Mechanism for transition from initial to stable cell-cell adhesion: Kinetic analysis of E-cadherin-mediated adhesion using a quantitative adhesion assay. J Cell Biol. 134: 549–557.

Bayas MV, Leung A, Evans E, Leckband D (2006). Lifetime measurements reveal kinetic differences between homophilic cadherin bonds. Biophys J. 90: 1385–1395.

Billett FS, Gould RP (1971). Fine structural changes in the differentiating epidermis of *Xenopus laevis* embryos. J Anat. 108: 465–480.

Boggon TJ, Murray J, Chappuis-Flament S, Wong E, Gumbiner BM, Shapiro L (2002). C-Cadherin ectodomain structure and implications for cell adhesion mechanisms. Science. 296: 1308–1313.

Bonitsis N, Batistatou A, Karantima S, Charalabopoulos K (2006). The role of cadherin/catenin complex in malignant melanoma. Exp Oncol. 28: 187–193.

Brady-Kalnay SM, Rimm DL, Tonks NK (1995). Receptor protein tyrosine phosphatase PTPμ associates with cadherins and catenins in vivo. J Cell Biol. 130: 977–986.

Casco VH, Izaguirre MF, Marin LM, Vergara MN, Lajmanovich RC, Peltzer P, Peralta Soler A (2006). Apoptotic cell death in the central nervous system of *Bufo arenarum* tadpoles induced by cypermethrin. Cell Biol Toxicol. 22: 199–211

Casco VH, Izaguirre MF, y Paz DA (1998). Efecto de los anticuerpos anti a-catenina sobre la embriogenesis de *Bufo arenarum. Bol Soc Biol Concepción*. 69: 55–61.

Casco VH, Izaguirre MF, Peralta Soler A, Paz DA (2000). Expression of polysialic acid, a- and b-catenins in adult toad testis in hibernation stage and after gonadotrophin-releasing hormone (GnRH) treatment. Eur J Morphol. 38: 167–175.

Castleman KR (1996). Digital Image Processing. Prentice Hall. New Jersey.

Chen WL, Lin CT, Lo HF, Lee JW, Tu IH, Hu FR. (2007). The role of protein tyrosine phosphorylation in the cell-cell interactions, junctional permeability and cell cycle control in post-confluent bovine corneal endothelial cells. Exp Eye Res. 85: 259–269.

Classen AK, Anderson KI, Marois E, Eaton S (2005). Hexagonal packing of *Drosophila* wing epithelial cells by the planar cell polarity pathway. Dev Cell. 9: 805–817.

Daniel JM, Reynolds AB (1995). The tyrosine kinase substrate p120cas binds directly to E-cadherin but not to the adenomatous polyposis coli protein or α-catenin. Mol Cell Biol. 15: 4819–4824.

Diaz-Zamboni JE (2004). Software para usuarios de microscopios de desconvolucion digital. Tesis de Grado (Inedito), Facultad de Ingenieria, Universidad Nacional de Entre Rios, Argentina.

Diaz-Zamboni JE, Adur JF, Vicente N, Fiorucci MP, Izaguirre MF, Casco VH (2008). 3D automatic quantification applied to optically sectioned images to improve microscopy analysis. Eur J Histochem. 52: 115–126.

Diaz-Zamboni JE, Paravani EV, Adur JF, Casco VH (2007). Implementation of an iterative deconvolution algorithm and its evaluation on three-dimensional images of fluorescence microscopy. Acta Microsc. 16: 8–15.

Esser S, Lampugnani MG, Corada M, Dejana E, Risau W (1998). Vascular endothelial growth factor induces VE-cadherin tyrosine phosphorylation in endothelial cells. J Cell Sci. 11: 1853–1865.

Fujita Y, Krause G, Scheffner M, Zechner D, Leddy HE, Behrens J, Sommer T, Birchmeier W (2002). Hakai, a c-Cbl-like protein, ubiquitinates and induces endocytosis of the E-cadherin complex. Nat Cell Biol. 4: 222–231.

Gosner KL (1960). A simplified table for staging anuran embryos and larvae with notes on identification. Herpetologica. 16: 183-190.

Gumbiner BM (2000). Regulation of cadherin adhesive activity. J Cell Biol. 148: 399–403.

Gumbiner B, Stevenson B, Grimaldi A (1988). The role of the cell adhesion molecule uvomorulin in the formation and maintenance of the epithelial junctional complex. J Cell Biol. 107: 1575–1587.

Hazan RB, Norton L (1998). The epidermal growth factor receptor modulates the interaction of E-cadherin with the actin cytoskeleton. J Biol Chem. 273: 9078–90784.

Hoschuetzky H, Aberle H, Kemler R (1994). Beta-catenin mediates the interaction of the cadherin-catenin complex with epidermal growth factor receptor. J Cell Biol. 127: 1375–1380.

Ito S, Karnovsky MJ (1968). Formaldehyde-glutaraldehyde fixatives containing trinitro compounds. J Cell Biol. 39: 168–169.

Izaguirre MF (2003). Influencia de la expresion de las moleculas de adhesion celular en el desarrollo embrionario, larval y metamorfico de Bufo arenarum. Tesis Doctoral (Inedita), Facultad de Bioquimica y Ciencias Biologicas, UNL, Argentina.

Izaguirre MF, Adur JF, Peralta Soler A, Casco VH (2001a). Alterations induced by E-cadherin and β-catenin antibodies during the development of *Bufo arenarum* (Anura–Bufonidae). Histol Hitopathol. 16: 1097–1106.

Izaguirre MF, Casco VH (2009). T3 regulates E-cadherin, and β- and α-catenin expression in stomach during metamorphosis of the toad *Rhinella arenarum*. Biotech. Histochem X: E-pub ahead of print.

Izaguirre MF, Garcia-Sancho MN, Miranda LA, Tomas J, Casco VH (2008). Influence of thyroid hormones on the expression of cell adhesion molecules in the developing kidney of *Bufo arenarum* tadpoles. Braz J Biol. 68: 631–637.

Izaguirre MF, Peralta Soler A, Casco VH (2000). Expression of NCAM-180 and N-cadherin during development in two South American anuran species (*Bufo arenarum* and *Hyla nana*). Eur J Histochem. 44: 407–418.

Izaguirre MF, Peralta Soler A, Lajmanovich RC, Casco VH (2001b). α-Catenin expression in the digestive tract of metamorphosing *Hyla nana* tadpoles (Anura, Hylidae): An immunohistochemical study. Amphibia Reptilia. 22: 256–261.

Izaguirre MF, Vergara MN, Casco VH (2006). Cas role in the brain apoptosis of *Bufo arenaum* induced by cypermethrin. BioCell. 30: 309–320.

Jensen PJ, Telegan B, Lavker RM, Wheelock MJ (1997). E-cadherin and P-cadherin have partially redundant roles in human epidermal stratification. Cell Tissue Res. 288: 307–316.

Kofron M, Heasman J, Lang SA, Wylie CC (2002). Plakoglobin is required for maintenance of the cortical actin skeleton in early *Xenopus* embryos and for cdc42-mediated wound healing. J Cell Biol. 158: 695–708.

Kusumi A, Suzuki K, Koyasako K (1999). Mobility and cytoeskeletal interactions of cell adhesion receptors. Curr Opin Cell Biol. 11: 582–590.

Lecuit T (2005). Adhesion remodeling underlying tissue morphogenesis. Trends Cell Biol. 15: 34–42.

Levi G, Gumbiner B, Thiery JP (1991). The distribution of E cadherin during *Xenopus laevis* development. Development. 111: 159–169.

McNally JG, Karpova T, Cooper J, Conchello JA (1999). Three-dimensional imaging by deconvolution microscopy. Methods. 19: 373–385.

McNeill HR, Ryan TA, Smith SJ, Nelson WJ (1993). Spatial and temporal dissection of immediate and early events following cadherin-mediated epithelial cell adhesion. J Cell Biol. 120: 1217–1226.

Miller JR, Moon RT (1996). Signal transduction through β-catenin and specification of cell fate during embryogenesis. Genes Dev. 10: 2527–2539.

Moles JP, Watt FM (1997). The epidermal stem cell compartment: Variation in expression levels of E-cadherin and catenins within the basal layer of human epidermis. J Histochem Cytochem. 45: 867–874.

Muller T, Choidas A, Reichmann E, Ullrich A (1999). Phosphorylation and free pool of beta-catenin are regulated by tyrosine kinases and tyrosine phosphatases during epithelial cell migration. J Biol Chem. 274: 10173–10183.

Nieset JE, Redfield AR, Jin F, Knudsen KA, Johnson KR, Wheelock MJ (1997). Characterization of the interaction of α-catenin with α-actinin and β-catenin/plakoglobin. J Cell Sci. 110: 1013–1022.

Palacios F, Tushir JS, Fujita Y, D'Souza-Schorey C (2005). Lysosomal targeting of E-cadherin: A unique mechanism for the down-regulation of cell-cell adhesion during epithelial to mesenchymal transitions. Mol Cell Biol. 25: 389–402.

Palovuori R, Sormunen R, Eskelinen S (2003). Src-induced disintegration of adherens junctions of madin-darby canine kidney cells is dependent on endocytosis of cadherin and antagonized by Tiam-1. Lab Invest. 83: 1901–1915.

Perl AK, Wilgenbus P, Dahl U, Semb H, Christofori G (1998). A causal role for E-cadherin in the transition from adenoma to carcinoma. Nature. 392: 190–193.

Perret E, Leung A, Feracci H, Evans E (2004). Trans-bonded pairs of E-cadherin exhibit a remarkable hierarchy of mechanical strengths. Proc Natl Acad Sci U S A. 47: 16472–16477.

Pokutta S, Weis WI (2007). Structure and mechanism of cadherins and catenins in cell-cell contacts. Annu Rev Cell Dev Biol. 23: 237–261.

Price VR, Reed CA, Lieberthal W, Schwartz JH (2002). ATP depletion of tubular cells causes dissociation of the zonula adherens and nuclear translocation of beta-catenin and LEF-1. J Am Soc Nephrol. 13: 1152–1161.

Rimm DL, Koslov ER, Kebriaei P, Cianci CD, Morrow JS (1995). Alpha1(E)-catenin is an actin-binding and -bundling protein mediating the attachment of Factin to the membrane adhesion complex. Proc Natl Acad Sci U S A. 92: 8813–8817.

Roitbak T, Ward CJ, Harris PC, Bacallao R, Ness SA, Wandinger-Ness A (2004). A polycystin-1 multiprotein complex is disrupted in polycystic kidney disease cells. Mol Biol Cell. 15: 1334–1346.

Staddon JM, Smales C, Schulze C, Esch FS, Rubin LL (1995). p120, a p120-related protein (p100), and the cadherin/catenin complex. J Cell Biol. 130: 369–381.

Steinert PM, Marekov LN (1999). Initiation of assembly of the cell envelope barrier structure of stratified squamous epithelia. Mol biol Cell. 10: 4247–4261.

Su LK, Vogelstein B, Kinzler KW (1993). Association of the APC tumor suppressor protein with catenins. Science. 262: 1734–1737.

Takeichi M, Nakagawa S, Aono S, Usui T, Uemura T (2000). Patterning of cell assemblies regulated by adhesion receptors of the cadherin superfamily. Philos Trans R Soc Lond B. 355: 885–890.

Tunggal JA, Helfrich I, Schmitz A, Schwarz H, Gunzel D, Fromm M, Kemler R, Krieg T, Niessen CM (2005). E-cadherin is essential for in vivo epidermal barrier function by regulating tight junctions. EMBO J. 24: 1146–1156.

Vleminckx K, Vakaet L, Jr., Mareel M, Fiers W, Van Roy F (1991). Genetic manipulation of E-cadherin expression by epithelial tumor cells reveals an invasion suppressor role. Cell 66: 107–119.

Wang Y, Nathans J (2007). Tissue/planar cell polarity in vertebrates: New insights and new questions. Development. 134: 647–658.

Waschke J (2008). The desmosome and pemphigus. Histochem Cell Biol. 130: 21–54.

Watabe M, Nagafuchi A, Tsukita S, Takeichi M. (1994). Induction of polarized cell-cell association and retardation of growth by activation of the E27 cadherin-catenin adhesion system in a dispersed carcinoma line. J Cell Biol. 127: 247–256.

Wheelock MJ, Kundsen KA, Johnson KR (1996). Membrane-cytoskeleton interaction with cadherin cell adhesion proteins: Roles of catenins as linker proteins. Curr Topics Memb. 43: 169–185.

Willert K, Jones KA (2006). Wnt signaling: Is the party in the nucleus? Genes Dev. 20: 1394–1404.

Xu W, Kimelman D (2007). Mechanistic insights from structural studies of beta-catenin and its binding partners. J Cell Sci. 120: 3337–3344.

Young BA, Sui X, Kiser TD, Hyun SW, Wang P, Sakarya S, Angelini DJ, Schaphorst KL, Hasday JD, Cross AS, Romer LH, Passaniti A, Goldblum SE (2003). Protein tyrosine phosphatase activity regulates endothelial cell-cell interactions, the paracellular pathway, and capillary tube stability. Am J Physiol Lung Cell Mol Physiol. 285: L63–L75.